

Spatio-Temporal Variation of Water Availability in a River Basin under CORDEX Simulated Future Projections

Jew Das¹ · N. V. Umamahesh¹

Received: 4 April 2017 / Accepted: 8 December 2017 /

Published online: 23 December 2017

© Springer Science+Business Media B.V., part of Springer Nature 2017

Abstract In the present study, spatio-temporal variability of hydrological components under climate change is analysed over Wainganga River basin, India. In order to address the climate change projection, hydrological modelling is carried out using a macro scale, semi-distributed three (3)-Layer Variable Infiltration Capacity (VIC-3 L) model. The high-resolution ($0.5^\circ \times 0.5^\circ$) meteorological variables are divided into multiple periods to calibrate and validate the VIC-3 L model. The future projections (2020–2094) of the water balance components are achieved using the high resolution hydrological variables from the COordinated Regional Downscaling EXperiment (CORDEX) dataset under Representative Concentration Pathway (RCP) 4.5 and 8.5 scenarios. The uncertainty associated with the multi-model projections are evaluated using Reliability Ensemble Averaging (REA) and the bias correction is accomplished with non-parametric quantile mapping. A probabilistic based areal drought index is also computed for different scenarios using Standardized Precipitation Evapotranspiration Index (SPEI). From the results, it is observed that amount of rainfall, evapotranspiration, and runoff has increased over the basin with no change in the spatial pattern. However, temporal variability is noticed with an increasing trend for rainfall and runoff in the non-monsoon season than the monsoon. Streamflow is expected to increase significantly, especially for medium to low flows (those occurring between 0.2 and 0.9 probability of exceedance in a Flow Duration Curve). In addition, the area under the drought condition has decreased under the projected climate scenarios.

Keywords CORDEX · Water balance · Reliability ensemble averaging · Drought index · Uncertainty analysis · VIC model

✉ N. V. Umamahesh
mahesh@nitw.ac.in

¹ Department of Civil Engineering, National Institute of Technology, Warangal, Telangana 506004, India

1 Introduction

The prevailing man made climate changes have an increasing influence on various systems of the earth climate. The fundamental nature of thermodynamics stated that change in temperature will have a significant influence on the thermal driven process (e.g. broadly hydrosphere and specifically the hydrological cycle) (IPCC 2014). Therefore, the climatic impacts will have prominent footprint on water cycle, precipitation patterns, water-holding capacity of atmosphere, evapotranspiration, infiltration, and surface runoff on spatial and temporal scales. In addition, the indirect impacts on water cycle induced due to the change in atmospheric circulation (Milly et al. 2015) also affect the regional changes in the hydro-climatic variables. The increasing human population and urbanization cause detrimental consequences (Uniyal et al. 2015) on natural resources like land and water. As the largest part of the available water is used for irrigation purposes, the alteration of hydrological events in terms of extremes (e.g. floods and droughts) leads to affect the crop yield (Abbaspour et al. 2009). Hence, there is an urgent need to assess the growing climate change impact on water resources over spatial and temporal scale for long-term strategic planning and better water management in future (Liuzzo et al. 2014; Mourato et al. 2015).

To assess the induced impact in future, Global Circulation Models (GCMs) are considered as most credible tools (Goharian et al. 2016). However, the vagueness of different GCMs' outputs is amplified as different models use different parameterization schemes, model structure, and response of the models to the atmospheric forcings (Teng et al. 2012). Moreover, the boundary conditions of the different models are different from each other so as the outputs even though they belong to the same experimental family (Srinivasa Raju et al. 2017). Therefore, it is advisable to incorporate multiple models with different scenarios in order to get the diversified climate change impact on hydro-climatic variables. As the decisions opted by the different GCMs increase the model complexity and ultimately the model simulations (Clark et al. 2016), hence the inter-model uncertainties are to be addressed through criteria based on the historical performance (Wilby 2010) before projecting for the future.

To evaluate the potential impact of climate change on water resources, hydrologic models have been proven an effective tool to inspect the climate change consequences by modifying the input information as projected by the climate models to get some indications about the characteristics of the water resources components (Liuzzo et al. 2014). In this sense, various studies have been carried out over different regions of the world to make an insight qualitative judgment on hydrological systems based on different climate change projections and some of the recent attempts are discussed as follows. Gosain et al. (2006) made very first attempt to assess the impact of climate change on hydrology of Indian rivers as a part of NATCOM (National Communication) project undertaken by the Ministry of Environmental and Forests, Government of India using Soil and Water Assessment Tool (SWAT). In their study, they advocated that the drought conditions may prevail in some parts of country whereas in other parts are predicted to face severe flood conditions under future climate scenarios. Later, Gosain et al. (2011) studied the spatio-temporal water availability in river systems in India and evaluated severity of floods and droughts using SWAT model. Moreover, they identified the vulnerable hotspots, which are more sensitive to the climate change. However, they have used only one climate model and the uncertainty associated with the climate models is not addressed in their study. Meenu et al. (2013) studied the future hydrological impact over Tunga-Bhadra river basin, India using statistically downscaled meteorological variables and Hydrologic Engineering Center's Hydrologic Modeling System version 3.4 (HEC-HMS 3.4). They used regression based downscaling to

downscale the GCM output and assessed the changes in the water balance components. However, regression based downscaling does not consider the regional features namely, land-atmosphere interactions that involves the mass and energy exchange between land and atmosphere (Wilby and Wigley 2000). Therefore, outputs from the dynamically downscaled GCM outputs could be a better choice, which incorporates the regional features at fine scale. A conceptual, Semi-distributed Land Used-based Runoff Processes (SLURP) hydrological model was used by Choi et al. (2014) over two river basins located in central Canada. The obtained results showed that seasonal variability of precipitation has significant impact on runoff. Moreover, they have emphasised the choice of downscaling methods than the choice of emission scenarios. In order to discretize the impact due to climate change and dynamic vegetation on runoff, Chawla and Mujumdar (2015) modeled the streamflow over upper Ganga basin in India using Variable Infiltration Capacity (VIC) model. With the obtained results, the authors reported that climate change has more prominent effect than the land use over the study area. Most recently, Khajeh et al. (2017) assessed the impact on hydrological drought over ZayandehRud River basin, Iran using a catchment scale rainfall-runoff model. Moreover, based on the drought analysis the results showed a prominent increase in the moderate, severe, and very severe drought levels as compared to the historical period. Similar to the above discussed studies, many recent studies show the application of different hydrological models to assess the impact. These include, but are not limited to Miller et al. (2012), Ravazzani et al. (2015), Li et al. (2015), Niraula et al. (2015), Teutschbein et al. (2015), Alam et al. (2016), Niu et al. (2017), Reshmidevi et al. (2017).

In the present study three (3)-Layer Variable Infiltration Capacity (VIC-3 L) model, a semi-distributed, macro scale, and grid based model, is used for hydrologic modelling. Because of its distributed nature with topographic, physiographic, and climatic controls, VIC is able to capture the regional variations in the hydrologic modelling. Moreover, VIC (Liang et al. 1994; Liang et al. 1996) incorporates the spatial variability of the region and has tested and applied over the years from large river basins (Abdulla et al. 1996; Wood et al. 1997; Zhu and Lettenmaier 2007) to continental and global scales (Nijssen et al. 2001; Shi et al. 2008). In addition, Hurkmans et al. (2010) clearly stated the advantages of VIC model such as 1) physically based evapotranspiration; 2) accumulation and melting process of snow; and 3) variations in the infiltration, land use, and elevation. Different studies have been carried out using VIC coupled with global models in the context of different climate change scenarios (Lu et al. 2013; Zhang et al. 2013; Yan et al. 2015) to forecast the streamflow pattern. Hence, VIC is used to assess the plausible variability in water balance components under future climate regimes.

In recent period, many studies are carried out over Indian river basins to evaluate the impact of climate change (Narsimlu et al. 2013; Uniyal et al. 2015; Alam et al. 2016; Das and Umamahesh 2016; Reshmidevi et al. 2017). However, incorporating the inter-modal uncertainty and areal drought index analysis will provide a better and effective evaluation of climate change. In this context, the present study is designed to analyse the spatio-temporal variability of water balance components over Wainganga river basin in India using a macro scale, grid based, and semi-distributed hydrologic model named as VIC-3 L model. As most parts of the study area opt for agriculture, it has become indispensable to evaluate and analyse the potential climate change impact for better adaptation strategies. The present study differs from other studies with the inclusion of Reliability Ensemble Averaging (REA) to minimize the uncertainty in multiple climate model outputs and processing of ensemble outputs with non-parametric quantile mapping prior to the hydrological modeling. Instead of considering a fixed and single calibration and validation period, the present study incorporates variable and multiple calibration and validation periods. In addition, authors have adopted a new approach

to evaluate the changeability in the water availability in terms of deficit and excess, which is accomplished by the probability, based areal drought index.

2 Methodology

In this study, authors have performed the impact assessment on water resources over a river basin using a semi-distributed hydrological model. Instead of using the multi-model outputs, different weights have been assigned based on performance and convergence criteria to different Regional Climate Models (RCMs). Bias correction is implemented to remove the systematic model errors for the weighted ensemble precipitation. Finally, the bias-corrected weighted variables are considered for further analysis, which quantifies the uncertainty associated with multi-model outputs. The atmospheric variables are then forced to generate the future streamflows from different climatic scenarios using VIC-3 L hydrologic model. To measure the performance of the VIC model we have performed multi-period calibration and validation instead of single period. Different hydrological components such as precipitation, evapotranspiration, and runoff over temporal as well as spatial scales are analysed. In addition, the drought events are investigated using multiscale drought indices and the probabilistic analysis of areal extent using severity-area curve for different scenarios. The proposed methodology is presented in the form of a flowchart in Fig. 1.

2.1 Study Area and Data Used

Wainganga sub-basin (Fig. 2) is located between $19^{\circ}30' \text{ N}$ - $22^{\circ}50' \text{ N}$ and $78^{\circ}0' \text{ E}$ - $81^{\circ}0' \text{ E}$, which is the largest sub-basin of one of the major river in India (Godavari River). The area of the basin is

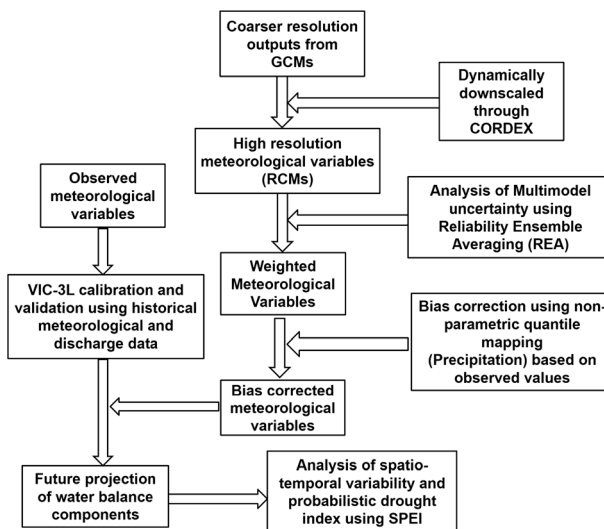


Fig. 1 Proposed Methodology

about 49,695.40 km² and the elevation of the study area above the mean sea level is ranging from 144 to 1036 m. The basin receives most of its rainfall during June to October (monsoon season). The annual depth of precipitation varies from 900 to 1600 mm, minimum temperature of the basin ranging from 7° C to 13 °C with maximum temperature from 39° C to 47 °C.

The meteorological variables such as precipitation, maximum and minimum temperature, and wind speed are obtained at a spatial resolution of (0.5° × 0.5°) i.e. ~50 km × 50 km and the location (29 grid points) of the meteorological variables are shown as grid points in Fig. 2. Precipitation and temperature data are collected from India Meteorological Department (IMD), whereas wind velocity is downloaded from Princeton University dataset (Sheffield et al. 2006) during 1971–2005. The high resolution gridded rainfall data was developed using more than 3000 rain gauge stations over India and the details of the data preparation is presented in Rajeevan and Bhate (2009). To validate the output from the hydrological model the streamflow data at the outlet of the Wainganga basin i.e. Asthi (Fig. 2) is obtained from Central Water Commission (CWC), Hyderabad from 1971 to 2005.

GCMs are most credible tools to project the future climate at a large scale; however, assessment of climate change signal at regional scale is necessary for proper adaptation. This requires finer spatial resolution, which incorporates the spatial variability such as dynamic land use and land cover, variability in soil and orography to improve the robustness of future climate projection. Hence, to project the future hydrology of the study area, outputs from the high resolution six GCMs (Table 1) are considered under the COordinated Regional Downscaling EXperiment (CORDEX) for the South Asia. The enhanced grid resolution of CORDEX enables the user to model more realistic regional climate response than the coarser grid resolution of GCM. Under this experiment, the atmospheric variables at coarser resolution from the GCMs are dynamically downscaled to the finer resolution and can be directly used for vulnerability, impacts, and adaptation studies under climate change (Gutowski et al. 2016). Therefore, the high-resolution GCMs are treated as RCMs in this study. The present study incorporates two climatic scenarios i.e. Representative Concentration Pathway (RCP) 4.5 and 8.5 (IPCC 2014) to evaluate the changes in different climatic forcings. RCP4.5 is considered as the stabilized radiative forcing

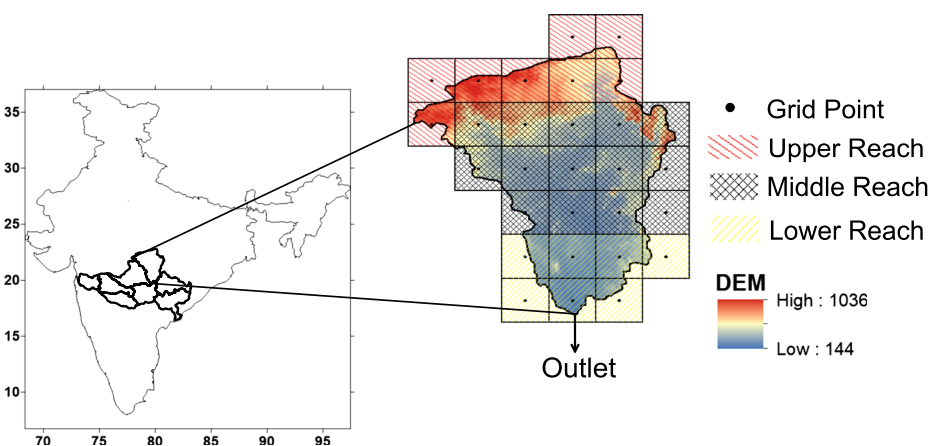


Fig. 2 Location map of the study area. Meteorological data are collected over the grid points and streamflow data are collected at the outlet named as Asthi

Table 1 Details of high resolution GCMs from the CORDEX project (Mcgregor and Dix 2001)

Experiment	Driving GCM	Institution
Commonwealth Australia Scientific and Industrial Research Organization, (CSIRO)	ACCESS1.0 (0.5°*0.5°)	CSIRO
Australia- CCAM	CNRM-CM5 (0.5°*0.5°)	Centre National de Recherches Météorologiques
	CCSM4 (0.5°*0.5°)	National Center for Atmospheric Research
	GFDL-CM3 (0.5°*0.5°)	Geophysical Fluid Dynamics Laboratory
	MPI-ESM-LR (0.5°*0.5°)	Max Planck Institute for Meteorology (MPI-M)
	NorESM1-M (0.5°*0.5°)	Norwegian Climate Centre

scenarios with CO₂ concentration of ~650 ppm at stabilization after 2100. RCP8.5 is considered as highest greenhouse gas emission scenario with CO₂ concentration of >1370 ppm in 2100. RCP4.5 and 8.5 are also known as intermediate emission and high emission scenarios respectively.

2.2 Climate Model Uncertainty

The climate models are the tools designed to assess the future climate scenarios incorporating the dynamic behaviour of the greenhouse gases. Hence, it is necessary to understand the strength and weakness of the models (Sengupta and Rajeevan 2013) through evaluating the ability of the model to capture the present climate (Sperber et al. 2013). The climate model projections are qualitative and hence given low level of confidence and high level of uncertainty (Visser et al. 2000). Therefore, quantification of the uncertainty is required to assess the future climate projection. In the present study, a quantitative method called as Reliability Ensemble Averaging (REA) is used to assign a justified weight to each model using performance and convergence criteria (Giorgi and Mearns 2002). This analysis assigns higher weight to more reliable models (Xu et al. 2010), which enables to minimize the uncertainty associated with the multi-model analysis. This quantitative and nonprobabilistic method was initially developed by Giorgi and Mearns (2002) and the probabilistic approach of this method was proposed by Giorgi and Mearns (2003). We have applied a Cumulative Distribution Functions (CDFs) based approach to evaluate the reliability criteria as previously performed by Chandra et al. (2015). REA is applied to all the atmospheric variables and weights are computed for RCP4.5, 8.5 and for all grid points. In REA, initial weights (Eq. 2) are obtained based on the ability of the RCMs to simulate the historical observations in term of Root Mean Square Error (RMSE) (Eq. 1), which defines the performance criteria.

$$RMSE = \left[\frac{1}{N} \sum_{i=1}^N (Observed_i - RCM_i) \right]^{1/2} \quad (1)$$

$$w_{int} = \frac{\left(\frac{1}{RMSE_i} \right)}{\left(\sum_{i=1}^n \frac{1}{RMSE_i} \right)} \quad (2)$$

To accomplish the convergence criteria weighted mean CDF is calculated by multiplying the initial weights with the future CDF value. Again, the RMSE is computed and the weights are assigned. This process is repeated until the obtained final weights for the different RCMs remain same as the previous iteration.

2.3 Bias Correction

Review of the previous studies has shown that post processing of the RCM output is recommended before providing as an input to the hydrological models (Teutschbein and Seibert 2010; Themeßl et al. 2011). The reasons behind the bias in the RCM outputs are studied and attributed in various studies (Teutschbein and Seibert 2010; Rauscher et al. 2010; Fiseha et al. 2014). Teutschbein and Seibert (2013) stated that outputs from high-resolution models show significant deviations because of systematic and random model errors. The bias associated with the precipitation, especially in the extreme events as a result of inadequate spatial resolution (Rauscher et al. 2010), causes difficulties in hydrological modelling (Argüeso et al. 2013). Gudmundsson et al. (2012) examined both parametric and non-parametric bias correction techniques to reduce the bias exclusively in the RCM precipitation using 82 precipitation stations. Based on the skill score they found the non-parametric transformation has better efficiency to reduce the systematic bias associated with precipitation.

Presently, after performing the REA analysis the weighted sum of the atmospheric variables (ensemble) for different grid points and different scenarios are extracted. The comparison between the observed and the ensemble revealed the better agreement with maximum and minimum temperature as well as wind speed. However, the precipitation (mostly the extreme) is highly underestimated. Hence, in the present study non-parametric quantile mapping as suggested by Gudmundsson et al. (2012) is used to correct the weighted precipitation series for the entire grid points using the Eq.3 and the correction is applied to the future period for all the grid points and scenarios.

$$P_{obs} = F_{obs}^{-1}(F_{wet}(P_{wet})) \quad (3)$$

where, P_{obs} and P_{wet} are observed and weighted precipitation, F_{wet} is the CDF of P_{wet} and F_{obs}^{-1} is the inverse CDF corresponding to P_{obs} .

2.4 Hydrological Model

The influence of climate change projections and internal dynamics of watershed can be efficiently achieved with diversified hydro-climatic variables through calibrated physically based, spatially distributed hydrological models (Mourato et al. 2015). In the present study, a semi-distributed, grid based, macro scale, VIC-3 L (Liang et al. 1994) is used to simulate the response of the catchment to produce streamflow under climate influenced atmospheric variables. This model is generally used in water resources modelling (Zhou et al. 2006), assessment of climate change impact (Yan et al. 2015), interaction between land and atmosphere (Zhu and Lettenmaier 2007). It includes both water and energy budgets and balances within the grid cell. VIC also incorporates land use variability, soil type, and non-linear base flow and it has different modules to generate the hydrological fluxes at each grid cell and simulate the streamflow at the outlet using convolution approach. The water balance equation used by VIC at each time step is given in Eq. 4.

$$\frac{\partial S}{\partial t} = P - E - R \quad (4)$$

where, $\partial S/\partial t$ is change in water storage, P is precipitation (mm), E is evapotranspiration (mm), and R is runoff in (mm). The VIC-3 L works in two parts, the initial part solves

the water and energy balance equations within the grid to compute different hydrologic components (Liang et al. 1994). The second part of the model transports the surface runoff within the grid cell to the outlet of the grid points and lastly routes the river channel to the basin outlet using the routing algorithm developed by Lohmann et al. (1998). Initially, grid-wise physical parameters (land use, soil type etc.) of the catchment are provided along with the meteorological files. As a result, the model provides the hydrological components (runoff, base flow, and evapotranspiration) in each grid cell. The outputs from the first module are given as an input to the final routing process; where the runoff generated in each grid is routed to the basin outlet. The controlling parameters in this module are flow direction file, flow fraction file, and station location file. In the present study, grid size of $0.5^{\circ} \times 0.5^{\circ}$ is used and monthly time step is considered to calibrate the VIC-3 L model.

In semi-distributed type hydrologic modelling, Land Use Land Cover (LULC) changes play an important role. Therefore, study, analysis, and understanding the changes in LULC of the study area are essential (Luo et al. 2016; Lu et al. 2013; Paul et al. 2016). Hence, the decadal changes in the LULC classification of the study area are examined for 1985, 1995, and 2005. The images are obtained at a resolution of 100 m (Roy et al. 2015) and can be download from http://daac.ornl.gov/cgi-bin/dsvviewer.pl?ds_id=1336.

The decadal LULC classification (Fig. 3) of the study area revealed that there was no significant change in the LULC patterns over last few decades. The results obtained from the LULC analysis is presented in Table 2. Based on the obtained results, it is assumed that the hydrological changes over the basin are altered due to the climate change.

The geology of the study area is mainly the granite and trap basalt rock. According to Food and Agriculture Organization (FAO), the dominant soil types are Lithosols and Chromic Vertisols. The soil classification of the study area is divided into (i) black soil, (ii) red soil, and (iii) mixed black and red soil. Moreover, in terms of soil type clay, clayey loam, and sandy loam soils dominate the study area. The soil texture in the study area is classified into medium and fine texture. The soil texture plays an important role in runoff generation. The larger texture produces less runoff and vice versa. The clay content is high in the study area, which reduces the pore space in the soil, restricts the movement of water through the soil, and increases the runoff.

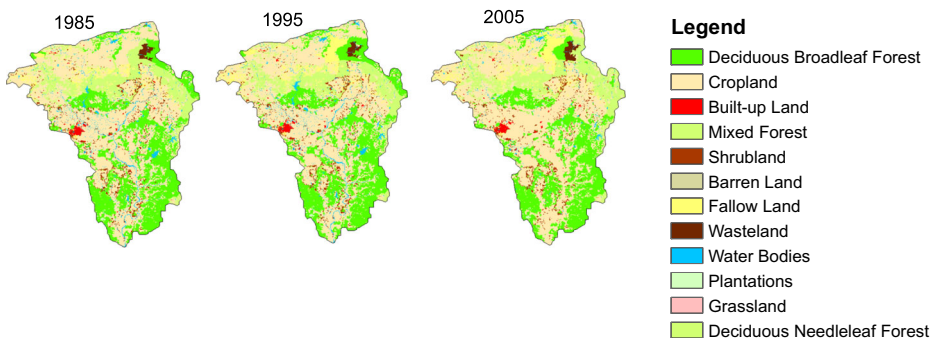


Fig. 3 LULC classification for 1985, 1995, and 2005 (Roy et al. 2015)

Table 2 Decadal LULC classification (percentage wise) (Roy et al. 2015)

Classification	1985	1995	2005
Deciduous Broadleaf Forest	26.11%	26.96%	24.46%
Cropland	49.30%	47.66%	48.94%
Built-up Land	0.69%	0.72%	0.73%
Mixed Forest	1.05%	1.06%	1.08%
Shrubland	3.20%	3.17%	3.00%
Barren Land	0.01%	0.02%	0.02%
Fallow Land	3.53%	5.49%	6.03%
Wasteland	0.63%	0.56%	0.74%
Water Bodies	2.68%	2.82%	1.09%
Plantations	0.26%	0.26%	0.28%
Grassland	0.001%	0.001%	0.001%
Deciduous Needleleaf Forest	12.49%	11.22%	13.59%

2.5 Drought Indices under Changing Climate

The remarkable sign of increases in temperature during past centuries and the future projections of increasing temperature profile during the twenty-first century by the climate change models are stated in several studies (for example: Jones and Moberg 2003; IPCC 2007a; Gosain et al. 2011; Asseng et al. 2014). The rise in temperature has drastic effect on the severity of droughts. Moreover, Loon (2015) stated that precipitation as well as temperature anomalies have significant effect on the drought development. To quantify, analyse, and monitor the drought events, different indices are commonly used such as Palmer Drought Severity Index (PDSI) (Palmer 1965; Liu et al. 2016; Muhammad et al. 2017) or Standardized Precipitation Index (SPI) (McKee et al. 1993; Hu et al. 2015; Zarch et al. 2015). However, the limitations of PDSI (subjectivity in indexing the drought conditions, spatial comparability) and SPI (based only on rainfall data) led to the development of new drought index named as Standardized Precipitation Evapotranspiration Index (SPEI) by Vicente-Serrano et al. (2010). The SPEI encompasses the temperature fluctuations like PDSI with the simplicity in calculation and multitemporal nature as SPI (Vicente-Serrano et al. 2010). The different strengths of the SPEI include; (1) it accounts the role of temperature change in drought conditions; (2) it is applicable to all climatic regions; (3) it is very useful in analysis of climate change impact under different future scenarios. In the present study, SPEI is used considering a 12-month aggregation time scale (SPEI-12) at each grid point. The procedures to compute the SPEI are as follows:

- Computation of the Potential Evapotranspiration (PET). Here, the monthly PET values for each grid point are obtained during the hydrological modelling using VIC-3 L (module-1).
- The difference (D) between precipitation and PET for each month is computed.
- The computed D values are aggregated based on the desired time scale (12 months in the present study).
- The suitable distribution for the D values are carried out by Vicente-Serrano et al. (2010) based on the most extreme values and they found the three parameter log-logistic distribution is suitable to standardize the D values to obtain the SPEI drought index.

The probability distribution function of the log-logistic distribution is given in Eq. 5.

$$F(x) = \left[1 + \left(\frac{\alpha}{x-\gamma} \right)^\beta \right]^{-1} \tag{5}$$

where, α , β , and γ are scale, shape and location parameters respectively. Then the SPEI is obtained by transforming the cumulative probability to the standard normal variate using the classical approximation proposed by Abramowitz and Stegun (1965).

$$SPEI = W - \frac{C_0 + C_1W + C_2W^2}{1 + d_1W + d_2W^2 + d_3W^3}; \tag{6}$$

$C_0 = 2.515517, C_1 = 0.802853, C_2 = 0.010328$
 $d_1 = 1.432788, d_2 = 0.189269, d_3 = 0.001308$

where, $W = \sqrt{-2\ln(P)}$ for $P \leq 0.5$; P is the exceeding probability of D and for $P > 0.5$ P is replaced by $1 - P$ and the resulting sign of SPEI is reversed.

2.6 SPEI-Based Probabilistic Drought Analysis

Drought analysis is important for assessing the impacts and effective planning of environmental and socioeconomic systems; however, assessment of probabilities and areal extent of drought severity add valuable information for proper planning and management (Bonaccorso et al. 2015). Hence, in the proposed study authors have used severity area curve proposed by Bonaccorso et al. (2015) to analyse the proportions of the study area which are below a fixed threshold value (i.e. SPEI drought indices). We have used the classification of SPEI drought indices as presented in Table 3 to categorize the wet and dry conditions.

The procedure to draw the severity area curve based on probabilistic approach is as follows.

- The desired aggregation of timescale based SPEI indices are computed as discussed earlier in sub-section 3.4 at each station. In the present study, we have computed SPEI-12 at all the grid points (m) as shown in Fig. 2.
- The area of influence is calculated for each grid point and is expressed as the fraction of the total study area(a_g).
- Then the SPEI-12 value ($S_{g,t}$) is computed at time (t) and at each grid point (g) for a given threshold value(S_o). The threshold value is varied from -3 to 3 with an increment of 0.5 .

Table 3 Classification of SPEI index (Vicente-Serrano et al. 2010; Ali et al. 2017)

SPEI Values	Interpretation
≥ 2.00	Extremely wet
1.50 to 1.99	Very wet
1.00 to 1.49	Moderately wet
-0.99 to 0.99	Near normal
-1.00 to -1.49	Moderately dry
-1.50 to -1.99	Severely dry
≤ -2.00	Extremely dry

- An indicator ($I_{g,t}$) with probability as shown in Eq. 7 is defined. Then the proportion of total area (A_t) below any threshold value (S_o) is computed using Eq. 8.

$$\begin{aligned}
 I_{g,t} &= 0 && \text{if } S_{g,t} > S_o \\
 I_{g,t} &= 1 && \text{if } S_{g,t} \leq S_o
 \end{aligned}
 \tag{7}$$

$$A_t(S_o) = \sum_{g=1}^m a_g \cdot I_{g,t}
 \tag{8}$$

3 Result and Discussions

3.1 Calibration and Validation of VIC Model

The VIC-3 L hydrologic model is calibrated and validated using the observed streamflow data at the outlet. Four different time windows, namely, 1971–1995, 1973–1997, 1975–1999, and 1978–2002 are considered for calibrating the model and remaining data are considered for validation. The hydrologic model response to the streamflow is controlled by the parameter set during the calibration period and in the present study the parameter ranges specified by Xie et al. (2007) are adopted. The range and obtained value of different parameters for different calibration periods are presented in Table 4. The parameters of VIC-3 L are computed based on trial and error method by changing the values of different parameters within the range. Generally, the multiple calibration is carried out to find out the transient behaviour of the parameters (Chawla and Mujumdar 2017) and the parameters are mainly depend on the physical characteristics of the region. Moreover, the effect of land use change has significant impact on soil properties (Gol 2009). As stated earlier, the LULC over the study area is not significantly changed and therefore, no significant variation in the parameters of the hydrological model is observed during different calibration periods. The efficiency of the model is evaluated using correlation coefficient (R) and Nash-Sutcliffe coefficient (NSE) for all the calibration periods. Among all the calibration periods, better R and NSE are obtained during calibration period 1978–2002 and calculated as 0.909 and 0.816 respectively. For the validation periods (1971–1977 and 2003–2005) combined R and NSE values are computed as 0.888 and 0.662 respectively. Graphical representation of the calibrated and validated flows is shown in Fig. 4.

3.2 Climate Change Impact Assessment

The calibrated VIC-3 L hydrological model is then forced to project the consequences of climate change on the hydrology of the study area. The historical period (1978–2002) is used

Table 4 Different parameters and their assigned value

Parameter	Description	Range	1978–2002	1975–1999	1973–1997	1971–1995
b_{mf}	Infiltration Parameter	0–10	6.0	6.2	6.0	6.1
D_s	Fraction of maximum baseflow	0–1	0.020	0.019	0.020	0.021
D_m	Maximum velocity of baseflow	0–30	0.1	0.1	0.1	0.1
W_s	Fraction of maximum soil moisture content	0–1	0.80	0.75	0.77	0.82
d_2	Second soil layer thickness	0.05–2	1.5	1.5	1.5	1.5
d_3	Third soil layer thickness	0.05–2	2	2	2	2

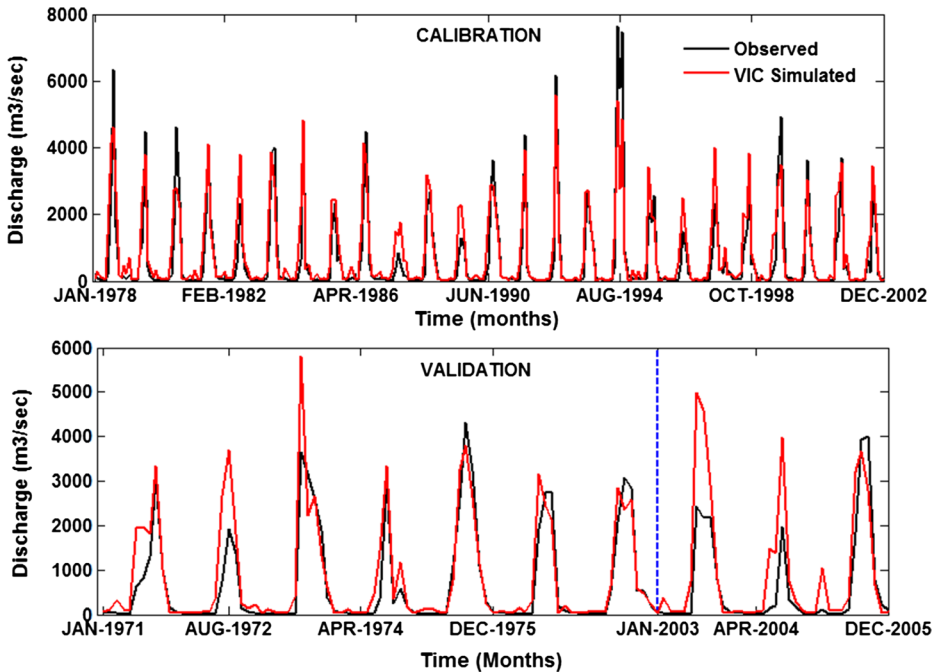


Fig. 4 Comparison of monthly streamflow for the calibration (upper panel) and validation (lower panel) periods. Blue line separates the two validation periods i.e. 1971–1977 and 2003–2005

as a baseline period to evaluate the future climate change of hydrological components. The future period is divided into three-time slices i.e. near (2020–2044), mid (2045–2069) and far (2070–2094) future. The spatial variability in annual rainfall, evapotranspiration (ET) and runoff are analysed over the basin as compared to the baseline period. Furthermore, the temporal variations of the hydrological variables are studied in monthly scale and the water availability is evaluated in terms of monthly Flow Duration Curve (FDC) by constructing seasonal and annual FDC variations.

3.2.1 Spatial Variability under Climate Change

The spatial distribution of annual mean precipitation, evapotranspiration, and runoff for the baseline period is presented in Fig. 5a. It can be noted that the annual precipitation ranges from 900 to 1600 mm, evapotranspiration varies from 400 to 550 mm and runoff throughout the basin is fluctuating between 400 to 750 mm. The upper reach of the basin is getting the minimum quantity of these hydrological variables and it is increasing gradually towards the lower reach of the basin.

Then each individual hydrologic component is analysed under different climate change scenarios and different time slices. Figure 5b represents the annual variability for precipitation in the future using stabilized (RCP4.5) and worst (RCP8.5) climate change scenarios. The distribution pattern is quite similar to the baseline period. For RCP4.5, annual precipitation varies from 600 to 2000 mm and in case of RCP8.5, it ranges from 970 to 2000 mm. The depth of rainfall increases from 2020 to 2094 for both the scenarios. Therefore, the upper limit of the annual precipitation is increased

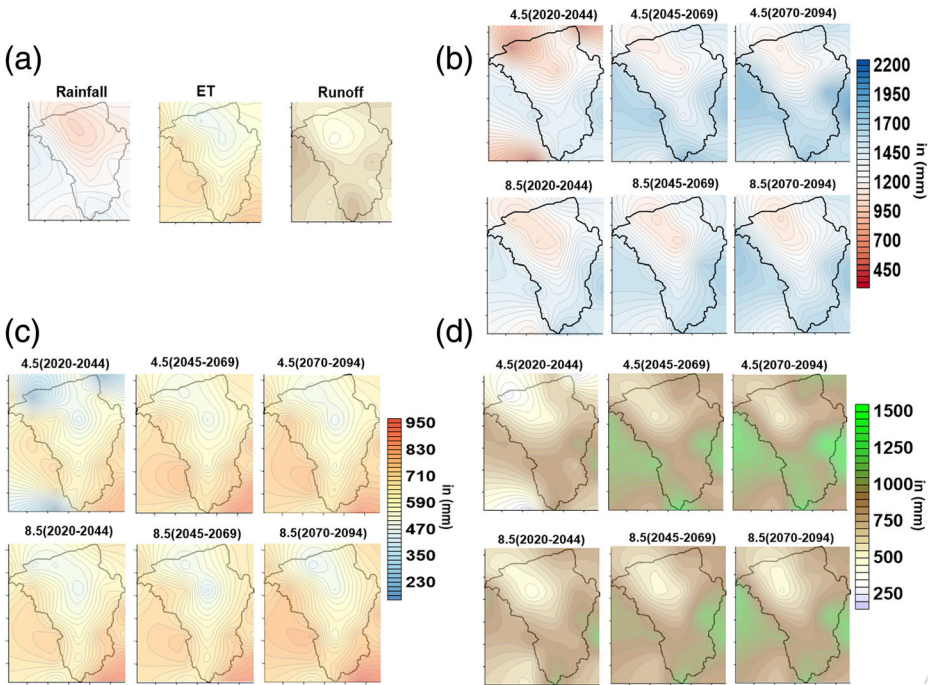


Fig. 5 **a** Spatial distribution of annual precipitation, ET, runoff for baseline; **b** Precipitation under RCP4.5 and RCP8.5; **c** ET under RCP4.5 and RCP8.5; **d** Runoff under RCP4.5 and RCP8.5. The colour scales of baseline precipitation, ET, and runoff 5 (a) are same as the respective precipitation, ET, and runoff for the future period and presented in 5(b), 5(c), and 5(d) respectively

by 25% and except RCP4.5 (2020–2044) where the lower limit also has decreased in future projections.

The spatial distribution of annual ET is depicted in Fig. 5c. The annual ET is increasing as compared to the observed baseline period. The maximum variation is noticed in RCP4.5 (2020–2044) and similar to the precipitation the ET is being intensified with the passage of time. The increase in ET can be attributed to the increase in the temperature due to the global warming. Solomon (1967) stated that increase in the ET is directly proportional to the change in the precipitation but at a slower rate. In the context of global warming, the water holding capacity of atmosphere increases with the increase in temperature resulting in increase in the precipitation amount (IPCC 2007b). In addition, Yang et al. (2016) attributed the declining trend in the ET to the declining trend of precipitation over the Loess Plateau, China. The spatial distributions of rainfall and ET in the present study also support the findings from the previous studies. The areas under high magnitude of the annual precipitation amount will have higher ET and vice versa for different periods and climatic scenarios. Similar kind of result was obtained by Mishra and Lilhare (2016) while evaluating the hydrologic sensitivity over the river basins in India. They stated that under global warming any increase in precipitation would lead to high ET and decline in precipitation will cause significant decrease in the ET over the Godavari Basin. However, the PET is very much sensitive to the change in the temperature rather than other climatic variables such as relative humidity, solar radiation, and wind speed (Guo et al. 2017).

Quantification of the water availability is necessary with respect to the proper allocation of water resources for domestic uses, agricultural uses etc. The annual average (standard deviation) of water balance components over the basin is computed for near, mid and far future under different scenarios. The historical average is 1216 mm (141 mm), 607 mm (81 mm), and 624 mm (93 mm) for precipitation, ET, and runoff respectively. The highest change in the mean is observed during far future than mid and near future for all the water balance components as compared to historical. Figure 5d shows the predicted runoff for different scenarios and it is observed that the runoff depth is increasing as compared to the baseline. Mostly the middle reaches and lower reaches are going to get more runoff. The runoff depth at upper reach during RCP4.5 (2020–2044) is significantly decreasing. The decrease in the runoff can be attributed to the significant decrease in the precipitation in upper reach during 2020–2044 as shown in Fig. 5b. Similar to the precipitation and ET the runoff depth is increasing towards the end of the century. Wang et al. (2013) examined the sensitivity of the runoff with precipitation and temperature under climate change forcings and showed that the runoff is more sensitive to the precipitation than temperature with nonlinear relation with the impact due to climate change. Also in the present study, the spatial distribution of the annual runoff is more sensitive to the precipitation pattern and it can be clearly observed during the period 2020–2044 under RCP4.5 scenario. During this period, the magnitude of the annual runoff in the upper reach of the basin is less and it can be attributed to the decrease in the depth of annual precipitation regardless lesser amount of ET.

The total basin is categorized into upper, middle, and lower reaches based on the elevation and presented in Fig. 2. The percentage change of the water balance components are evaluated based on the historical period for the different climate change scenarios and different reaches. The percentage change is computed based on annual values. The average percentage change in rainfall for lower, middle, and upper reaches are 34%, 31%, and 11% under RCP4.5 and 36%, 29%, and 16% under RCP8.5 respectively. Similarly, average percentage changes in ET for lower, middle, and upper reaches are 21%, 11%, and -6% under RCP4.5 and 26%, 13%, and 2% under RCP8.5 respectively. The average percentage change in runoff for lower, middle, and upper reaches are 42%, 47%, and 24% under RCP4.5 and 41%, 40%, and 27% under RCP8.5. The mean percentage of increase in ET is higher in case of RCP8.5 than RCP4.5 due to the higher emissions under RCP8.5, which are going to increase the temperature significantly. Moreover, the change in the runoff in the lower reach is influenced due to the local changes as well as the change observed in the upper and middle reaches. Hence, the impact of climate change is going to intensify the hydrological variables with respect to the historical period.

3.2.2 Temporal Variability under Climate Change

Temporal analysis of the hydrological variables is carried out on monthly basis to identify the seasonal changes for the future projection. Temporal variation of precipitation, ET, and runoff are plotted as boxplot and presented in Fig. 6a–c respectively. The monthly variation in precipitation pattern shows a significant increase in the rainfall depth over the non-monsoon period. The precipitation depth is also increasing in the month of June i.e. onset of the monsoon as compared to the baseline period. However, in the month of August and September the precipitation amount has decreased significantly, which will affect the total monsoon precipitation. The decrease or shift in the monsoon rainfall was studied by Annamalai et al. (2013). In their study, they attributed the decrease in the monsoon rainfall to the increase in the western Indian Ocean sea level pressure and weakening of low-level monsoon winds. This

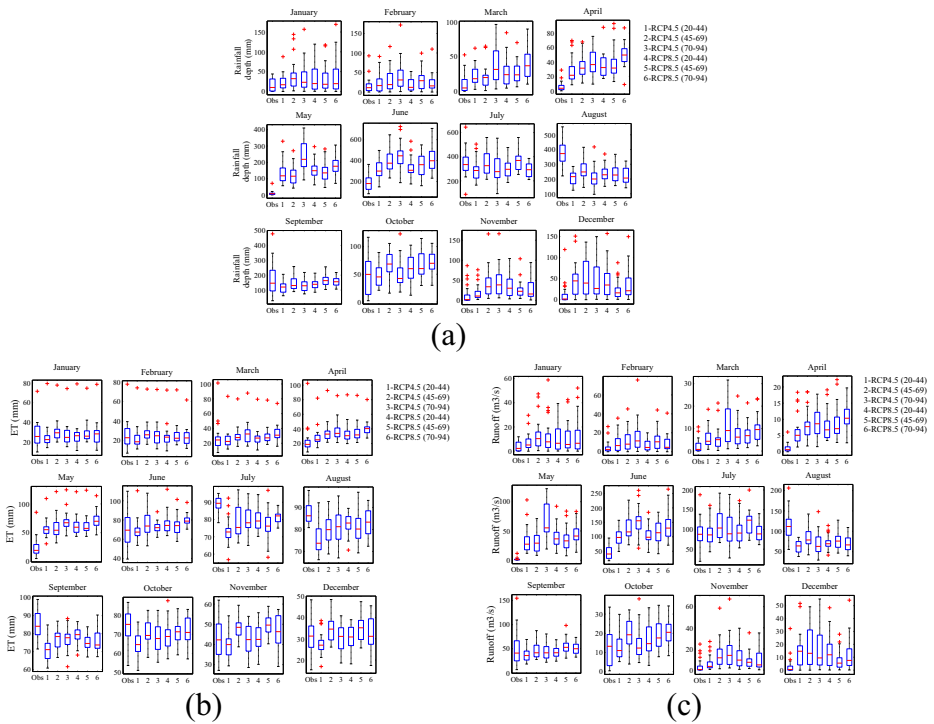


Fig. 6 Monthly variation for RCP4.5 and 8.5 over the basin **(a)** Precipitation; **b** ET; **c** Runoff

circulation patterns are dynamically consistent over India and resulting in decreasing total cloud amount. In addition, they have noted the drying trend in the regional seasonal mean (June–September) related with South Asian summer monsoon. The increase in Sea Surface Temperature (SST) due to the global warming effects the monsoon convection differently and brings more precipitation to the western Pacific and less to the South Asia (Annamalai et al. 2013). The upper extreme of the ET has increased in the month of April and May whereas in case of other months the upper extreme is equal or less than the baseline period. The runoff has increased during non-monsoon season and follows a similar kind of variation as observed in case of precipitation. Hence, with the evidence from the spatial and temporal distribution, it can be concluded that runoff varies significantly with the precipitation than ET over the basin.

In order to compute the water availability of the study area, FDC under different scenarios is plotted using VIC simulated future flows. The FDC specifies the flow that may be exceeded at a given level of probability and this analysis help in designing of hydrological structures like culverts, dam, and drainage networks, etc. Monthly and seasonal FDCs are constructed under RCP4.5 and 8.5 scenarios. Figure 7 represents the FDCs at the Wainganga basin outlet. From the plots, it is noted that monthly and seasonal flows show an overall increase for both the scenarios except the near future under RCP8.5 for the non-monsoon season as compared to the baseline period. From Fig. 7, it is also noticed that the flows with probability of exceedance between 0.2 and 0.9 have increased significantly as compared to the historical period. The increase in the probability of medium and low flows may influence the groundwater volume significantly as stated by Fiseha et al. (2014). Unlike the RCP8.5, a gradual increase of water availability with passage of time is noticed under RCP4.5. The LULC variations are kept

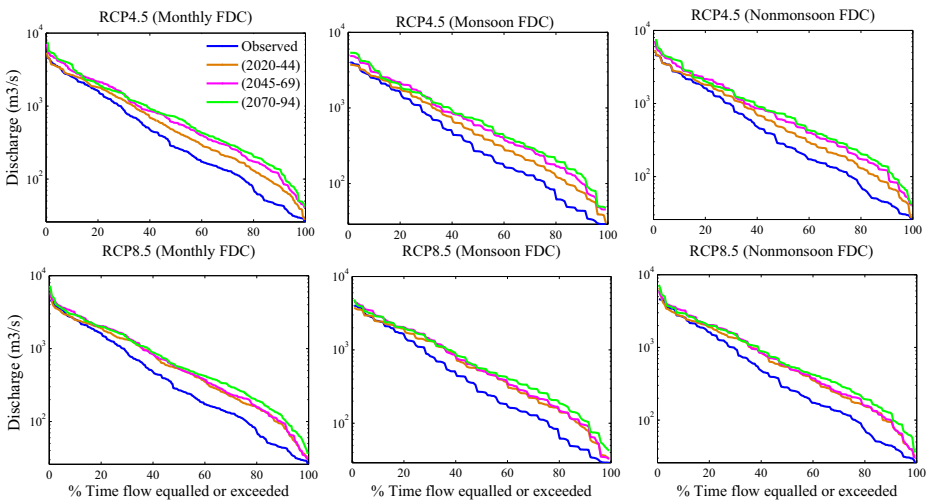


Fig. 7 Temporal variations in FDC at the outlet of the study area. The upper and lower panels represent RCP 4.5 and 8.5 respectively

constant based on Table 2; however, in future the alternation of the LULC in the study area can be considered with uncertainties for additional usage.

Drought analysis is carried out over the basin using SPEI and probability based areal index as described in Section 2. For example, Fig. 8a shows severity area curve for the January

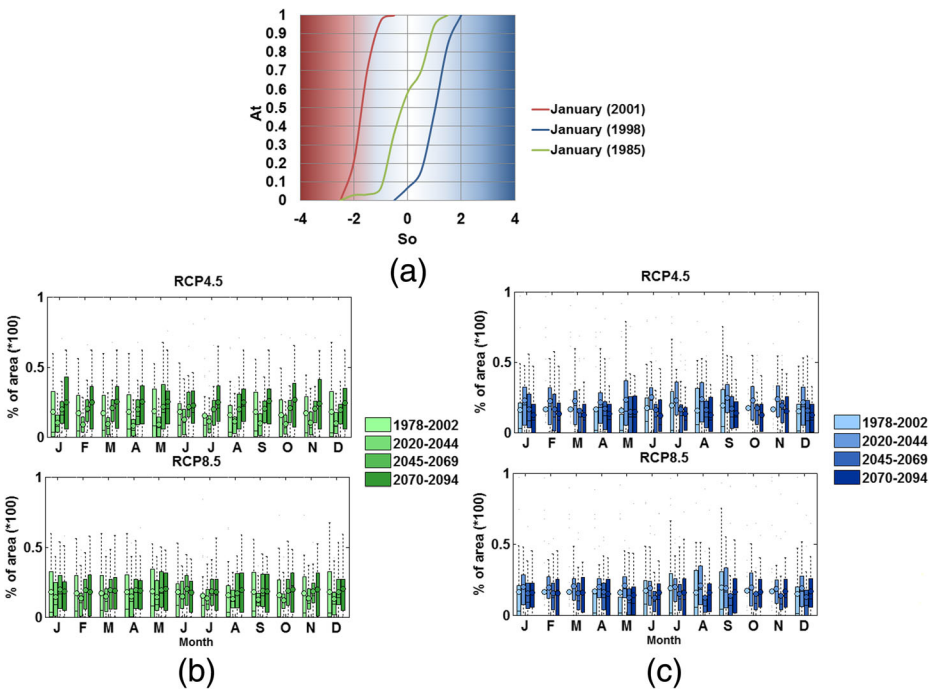


Fig. 8 a Severity-area curves for January month of different years; Month-wise areal extent associated (b) with ≥ 1 and (c) with ≤ -1

month of historical period with the reference to the SPEI-12. It represents the drought conditions that occurred in January month in different years. In particular, the curve associated with the January (2001) states that about 97% of the total area was affected by drought conditions ($S_o \leq -1$); whereas, in January (1998) about 50% area was under near normal condition and 50% area was under wet conditions. In January (1985) most of the area of the Wainganga basin was under normal conditions.

From Table 3, it can be noted that the normal condition is specified between the ranges of -0.99 to 0.99 ; hence, we have considered -1 and 1 as two borders for the drought and excess conditions respectively. The total area below -1 and above 1 is computed for the historical as well as future period under different scenarios and presented in Fig. 8c, b respectively. The circle (o) in the boxplots represents the average area for the particular time span. It can be noted from Fig. 8c that, average area under the drought condition is increasing for the near future with respect to the historical period for both the RCP scenarios. However, the average drought prone area percentage for the mid and far future is decreasing for RCP4.5 and 8.5. In addition, the influence of the different climate scenarios has been observed from the month January to May where areal extent of drought conditions is significantly high under RCP4.5 than RCP8.5.

A similar study has been carried out to analyse the areal extent under wet condition for different climate scenarios and for the future projection (Fig. 8b). It is noted that the mean average areal extent for the near future under both the scenarios showing decrease in the wet condition as compared to the historical series. Nevertheless, the mean areal wet condition for the mid and far future is increased gradually and the far future is showing the highest increase in the mean areal extent of the wet condition. The change in the monthly areal average for the future projection is gradual under RCP8.5; however, the change is abrupt in case of RCP4.5.

Hence, implementing the inter-modal uncertainty with bias correction, the outcomes should be considered as indicative about the response of the hydrological regime to the climate change rather than conclusive. By incorporating finer resolution climatic variables with physically based distributed hydrological model, the results from the present investigation can be utilized to develop adaptation strategies with the increasing pace of climate change. Encompassing the climate scenario uncertainty and comparing with other hydrological models can be resulted more reliable outcomes to improve the robustness of planning and management decisions.

4 Summary and Conclusions

This study analyses the impact of climate change forcings on water balance components of Wainganga River basin using dynamically downscaled GCMs to finer resolution of $0.5^0 \times 0.5^0$ under CORDEX for the South Asia. The multi-model uncertainties are quantified through REA and the post processing of the high-resolution outputs is carried out using bias correction. Then the calibrated VIC-3 L hydrological model, using the historical data from IMD, is forced to project the streamflow for the future under RCP4.5 and 8.5 scenarios. Finally, the spatial and temporal variations in hydrological components and the probabilistic areal extent of the drought events are analyzed. The critical findings of the study are presented as follows.

- The annual spatial variations of precipitation, ET, and runoff have increased over the basin as compared to the baseline period and runoff of the basin is more sensitive to the precipitation. However, the spatial distribution patterns remain similar to the historical pattern.

- Based on the future scenarios, the depth of precipitation may increase during non-monsoon than monsoon period.
- The enhancement in the water availability in the basin has been found in terms of FDC. Probability of exceedance between 0.2 and 0.9 has increased significantly as compared to the historical period, which will influence the groundwater volume in the study area.
- The average areal extent of the drought conditions under both scenarios are going to decrease. In contrast, the wet conditions of the basin are projected to increase.

Acknowledgements The authors thank the anonymous reviewers for their constructive comments and suggestions for improving the quality of the manuscript.

References

- Abbaspour KC, Faramarzi M, Ghasemi SS, Yang H (2009) Assessing the impact of climate change on water resources in Iran. *Water Resour Res* 45:1–16. <https://doi.org/10.1029/2008WR007615>
- Abdulla FA, Lettenmaier DP, Wood EF, Smith JA (1996) Application of a macroscale hydrologic model to estimate the water balance of the Arkansas-Red River basin. *J Geophys Res Atmos* 101:7449–7459. <https://doi.org/10.1029/95JD02416>
- Abramowitz M, Stegun IA (1965) Handbook of mathematical functions. National Bureau of Standards, Applied Mathematics Series, Washington, D.C.
- Alam S, Ali MM, Islam Z (2016) Future streamflow of Brahmaputra River basin under synthetic climate change scenarios. *J Hydrol Eng* 21:5016027. [https://doi.org/10.1061/\(ASCE\)HE.1943-5584.0001435](https://doi.org/10.1061/(ASCE)HE.1943-5584.0001435)
- Ali Z, Hussain I, Faisal M et al (2017) A novel multi-scalar drought index for monitoring drought: the standardized precipitation temperature index. *Water Resour Manag*. <https://doi.org/10.1007/s11269-017-1788-1>
- Annamalai H, Hafner J, Sooraj KP, Pillai P (2013) Global warming shifts the monsoon circulation, drying South Asia. *J Clim* 26:2701–2718. <https://doi.org/10.1175/JCLI-D-12-00208.1>
- Argüeso D, Evans JP, Fita L (2013) Precipitation bias correction of very high resolution regional climate models. *Hydrol Earth Syst Sci* 17:4379–4388. <https://doi.org/10.5194/hess-17-4379-2013>
- Asseng S, Ewert F, Martre P et al (2014) Rising temperatures reduce global wheat production. *Nat Clim Chang* 5: 143–147. <https://doi.org/10.1038/nclimate2470>
- Bonaccorso B, Peres DJ, Castano A, Cancelliere A (2015) SPI-based probabilistic analysis of drought areal extent in Sicily. *Water Resour Manag* 29:459–470. <https://doi.org/10.1007/s11269-014-0673-4>
- Chandra R, Saha U, Mujumdar PP (2015) Model and parameter uncertainty in IDF relationships under climate change. *Adv Water Resour* 79:127–139. <https://doi.org/10.1016/j.advwatres.2015.02.011>
- Chawla I, Mujumdar PP (2015) Isolating the impacts of land use and climate change on streamflow. *Hydrol Earth Syst Sci* 19:3633–3651. <https://doi.org/10.5194/hess-19-3633-2015>
- Chawla I, Mujumdar PP (2017) Partitioning uncertainty in streamflow projections under nonstationary model conditions. *Adv Water Resour*. <https://doi.org/10.1016/j.advwatres.2017.10.013>
- Choi W, Kim SJ, Lee M et al (2014) Hydrological impacts of warmer and wetter climate in Troutlake and Sturgeon River basins in Central Canada. *Water Resour Manag* 28:5319–5333. <https://doi.org/10.1007/s11269-014-0803-z>
- Clark MP, Wilby RL, Gutmann ED et al (2016) Characterizing uncertainty of the hydrologic impacts of climate change. *Curr Clim Chang Reports* 2:55–64. <https://doi.org/10.1007/s40641-016-0034-x>
- Das J, Umamahesh NV (2016) Downscaling monsoon rainfall over river Godavari Basin under different climate-change scenarios. *Water Resour Manag* 30:5575–5587. <https://doi.org/10.1007/s11269-016-1549-6>
- Fischa BM, Setegn SG, Melesse AM et al (2014) Impact of climate change on the hydrology of upper Tiber River basin using bias corrected regional climate model. *Water Resour Manag* 28:1327–1343. <https://doi.org/10.1007/s11269-014-0546-x>
- Giorgi F, Mearns LO (2002) Calculation of average, uncertainty range, and reliability of regional climate changes from AOGCM simulations via the “reliability ensemble averaging” (REA) method. *J Clim* 15:1141–1158. [https://doi.org/10.1175/1520-0442\(2002\)015<1141:COAURA>2.0.CO;2](https://doi.org/10.1175/1520-0442(2002)015<1141:COAURA>2.0.CO;2)
- Giorgi F, Mearns LO (2003) Probability of regional climate change based on the reliability ensemble averaging (REA) method. *Geophys Res Lett* 30:2–5. <https://doi.org/10.1029/2003GL017130>

- Goharian E, Burian SJ, Bardsley T, Strong C (2016) Incorporating potential severity into vulnerability assessment of water supply systems under climate change conditions. *J Water Resour Plan Manag* 142:4015051. [https://doi.org/10.1061/\(ASCE\)WR.1943-5452.0000579](https://doi.org/10.1061/(ASCE)WR.1943-5452.0000579)
- Gol C (2009) The effects of land use change on soil properties and organic carbon at Dagdami river catchment in Turkey. *J Environ Biol* 30:825–830
- Gosain AK, Rao S, Basuray D (2006) Climate change impact assessment on hydrology of Indian river basins. *Curr Sci* 90:346–353
- Gosain AK, Rao S, Arora A (2011) Climate change impact assessment of water resources of India. *Curr Sci* 101: 356–371
- Gudmundsson L, Bremnes JB, Haugen JE, Engen-Skaugen T (2012) Technical note: downscaling RCM precipitation to the station scale using statistical transformations – a comparison of methods. *Hydrol Earth Syst Sci* 16:3383–3390. <https://doi.org/10.5194/hess-16-3383-2012>
- Guo D, Westra S, Maier HR (2017) Sensitivity of potential evapotranspiration to changes in climate variables for different Australian climatic zones. *Hydrol Earth Syst Sci* 21:2107–2126. <https://doi.org/10.5194/hess-21-2107-2017>
- Gutowski JW, Giorgi F, Timbal B et al (2016) WCRP COordinated regional downscaling EXperiment (CORDEX): a diagnostic MIP for CMIP6. *Geosci Model Dev* 9:4087–4095. <https://doi.org/10.5194/gmd-9-4087-2016>
- Hu Y-M, Liang Z-M, Liu Y-W et al (2015) Uncertainty analysis of SPI calculation and drought assessment based on the application of bootstrap. *Int J Climatol* 35:1847–1857. <https://doi.org/10.1002/joc.4091>
- Hurkmans R, Terink W, Uijlenhoet R et al (2010) Changes in streamflow dynamics in the Rhine Basin under three high-resolution regional climate scenarios. *J Clim* 23:679–699. <https://doi.org/10.1175/2009JCLI3066.1>
- IPCC (2007a) Climate change 2007: Impacts, adaptation and vulnerability. In: Parry ML, et al (eds). Contribution of Working Group II to the Fourth Assessment Report of the Intergovernmental Panel on Climate Change. Cambridge University Press, Cambridge, pp 976. https://www.ipcc.ch/pdf/assessment-report/ar4/wg2/ar4_wg2_full_report.pdf
- IPCC (2007b) Climate change 2007: the physical science basis. *Intergov Panel Clim Chang* 446:727–728. <https://doi.org/10.1038/446727a>
- IPCC (2014) Climate change 2014: synthesis report. Contribution of Working Groups I, II and III to the Fifth Assessment Report of the Intergovernmental Panel on Climate Change
- Jones PD, Moberg A (2003) Hemispheric and large-scale surface air temperature variations: an extensive revision and an update to 2001. *J Clim* 16:206–223. [https://doi.org/10.1175/1520-0442\(2003\)016<0206:HALSSA>2.0.CO;2](https://doi.org/10.1175/1520-0442(2003)016<0206:HALSSA>2.0.CO;2)
- Khajeh S, Paimozd S, Moghaddasi M (2017) Assessing the impact of climate changes on hydrological drought based on reservoir performance indices (case study: ZayandehRud River basin, Iran). *Water Resour Manag* 31:2595–2610. <https://doi.org/10.1007/s11269-017-1642-5>
- Li L, Zhang L, Xia J et al (2015) Implications of modelled climate and land cover changes on runoff in the middle route of the south to north water transfer project in China. *Water Resour Manag* 29:2563–2579. <https://doi.org/10.1007/s11269-015-0957-3>
- Liang X, Lettenmaier DP, Wood EF, Burges SJ (1994) A simple hydrologically based model of land surface water and energy fluxes for general circulation models. *J Geophys Res* 99:14415. <https://doi.org/10.1029/94JD00483>
- Liang X, Wood EF, Lettenmaier DP (1996) Surface soil moisture parameterization of the VIC-2L model: evaluation and modification. *Glob Planet Chang* 13:195–206. [https://doi.org/10.1016/0921-8181\(95\)00046-1](https://doi.org/10.1016/0921-8181(95)00046-1)
- Liu Y, Ren L, Hong Y et al (2016) Sensitivity analysis of standardization procedures in drought indices to varied input data selections. *J Hydrol* 538:817–830. <https://doi.org/10.1016/j.jhydrol.2016.04.073>
- Liuzzo L, Noto LV, Amone E et al (2014) Modifications in water resources availability under climate changes: a case study in a Sicilian Basin. *Water Resour Manag* 29:1117–1135. <https://doi.org/10.1007/s11269-014-0864-z>
- Lohmann D, Raschke E, Nijssen B, Lettenmaier DP (1998) Regional scale hydrology: II. Application of the VIC-2L model to the Weser River, Germany. *Hydrol Sci J* 43:143–158. <https://doi.org/10.1080/02626669809492108>
- Loon AFV (2015) Hydrological drought explained. *Wiley Interdiscip Rev Water* 2:359–392. <https://doi.org/10.1002/wat2.1085>
- Lu G-H, Xiao H, Wu Z-Y et al (2013) Assessing the impacts of future climate change on hydrology in Huang-Huai-Hai region in China using the PRECIS and VIC models. *J Hydrol Eng* 18:1077–1087. [https://doi.org/10.1061/\(ASCE\)HE.1943-5584.0000632](https://doi.org/10.1061/(ASCE)HE.1943-5584.0000632)
- Luo K, Tao F, Moiwu JP, Xiao D (2016) Attribution of hydrological change in Heihe River Basin to climate and land use change in the past three decades. *Sci Rep* 6:33704. <https://doi.org/10.1038/srep33704>
- Mcgregor JL, Dix MR (2001) The CSIRO conformal-cubic atmospheric GCM. In: IUTAM symposium on advances in mathematical modelling of atmosphere and ocean dynamics, 21. Fluid Mechanics and Its Applications. Springer, Dordrecht, pp 197–202. https://doi.org/10.1007/978-94-010-0792-4_25

- Mckee TB, Doesken NJ, Kleist J (1993) The relationship of drought frequency and duration to time scales. *AMS 8th Conf Appl Climatol* 179–184
- Meenu R, Rehana S, Mujumdar PP (2013) Assessment of hydrologic impacts of climate change in Tunga-Bhadra river basin, India with HEC-HMS and SDSM. *Hydrol Process* 27:1572–1589. <https://doi.org/10.1002/hyp.9220>
- Miller WP, Butler RA, Piechota T et al (2012) Water management decisions using multiple hydrologic models within the San Juan River basin under changing climate conditions. *J Water Resour Plan Manag* 138:412–420. [https://doi.org/10.1061/\(ASCE\)WR.1943-5452.0000237](https://doi.org/10.1061/(ASCE)WR.1943-5452.0000237)
- Milly PCD, Betancourt J, Falkenmark M et al (2015) On critiques of “stationarity is dead: whither water management?”. *Water Resour Res* 51:7785–7789. <https://doi.org/10.1002/2015WR017408>
- Mishra V, Lihare R (2016) Hydrologic sensitivity of Indian sub-continental river basins to climate change. *Glob Planet Change* 139:78–96. <https://doi.org/10.1016/j.gloplacha.2016.01.003>
- Mourato S, Moreira M, Corte-Real J (2015) Water resources impact assessment under climate change scenarios in Mediterranean watersheds. *Water Resour Manag* 29:2377–2391. <https://doi.org/10.1007/s11269-015-0947-5>
- Muhammad A, Kumar Jha S, Rasmussen PF (2017) Drought characterization for a snow-dominated region of Afghanistan. *J Hydrol Eng* 22:5017014. [https://doi.org/10.1061/\(ASCE\)HE.1943-5584.0001543](https://doi.org/10.1061/(ASCE)HE.1943-5584.0001543)
- Narsimlu B, Gosain AK, Chahar BR (2013) Assessment of future climate change impacts on water resources of upper Sind River basin, India using SWAT model. *Water Resour Manag* 27:3647–3662. <https://doi.org/10.1007/s11269-013-0371-7>
- Nijssen B, Schnur R, Lettenmaier DP (2001) Global retrospective estimation of soil moisture using the variable infiltration capacity land surface model, 1980–93. *J Clim* 14:1790–1808. [https://doi.org/10.1175/1520-0442\(2001\)014<1790:GREOSM>2.0.CO;2](https://doi.org/10.1175/1520-0442(2001)014<1790:GREOSM>2.0.CO;2)
- Niraula R, Meixner T, Norman LM (2015) Determining the importance of model calibration for forecasting absolute/relative changes in streamflow from LULC and climate changes. *J Hydrol* 522:439–451. <https://doi.org/10.1016/j.jhydrol.2015.01.007>
- Niu J, Chen J, Wang K, Sivakumar B (2017) Multi-scale streamflow variability responses to precipitation over the headwater catchments in southern China. *J Hydrol* 551:14–28. <https://doi.org/10.1016/j.jhydrol.2017.05.052>
- Palmer WC (1965) Meteorological drought. U.S. weather bur. Res. Pap. No. 45-58. U.S. Weather Bureau, Washington, D.C.
- Paul S, Ghosh S, Oglesby R et al (2016) Weakening of Indian summer monsoon rainfall due to changes in land use land cover. *Sci Rep* 6:32177. <https://doi.org/10.1038/srep32177>
- Rajeevan M, Bhate J (2009) A high resolution daily gridded rainfall dataset (1971-2005) for mesoscale meteorological studies. *Curr Sci* 96:558–562
- Rauscher SA, Coppola E, Piani C, Giorgi F (2010) Resolution effects on regional climate model simulations of seasonal precipitation over Europe. *Clim Dyn* 35:685–711. <https://doi.org/10.1007/s00382-009-0607-7>
- Ravazzani G, Barbero S, Salandini A et al (2015) An integrated hydrological model for assessing climate change impacts on water resources of the upper Po River basin. *Water Resour Manag* 29:1193–1215. <https://doi.org/10.1007/s11269-014-0868-8>
- Reshmidevi TV, Nagesh Kumar D, Mehrotra R, Sharma A (2017) Estimation of the climate change impact on a catchment water balance using an ensemble of GCMs. *J Hydrol*. <https://doi.org/10.1016/j.jhydrol.2017.02.016>
- Roy P, Roy A, Joshi P et al (2015) Development of decadal (1985–1995–2005) land use and land cover database for India. *Remote Sens* 7:2401–2430. <https://doi.org/10.3390/rs70302401>
- Sengupta A, Rajeevan M (2013) Uncertainty quantification and reliability analysis of CMIP5 projections for the Indian summer monsoon. *Curr Sci* 105:1692–1703
- Shi X, Wood AW, Lettenmaier DP (2008) How essential is hydrologic model calibration to seasonal streamflow forecasting? *J Hydrometeorol* 9:1350–1363. <https://doi.org/10.1175/2008JHM1001.1>
- Sheffield J, Goteti G, Wood EF (2006) Development of a 50-year high-resolution global dataset of meteorological forcings for land surface modeling. *J Clim* 19:3088–3111. <https://doi.org/10.1175/JCLI3790.1>
- Solomon S (1967) Relationship between precipitation, evaporation, and runoff in tropical equatorial regions. *Water Resour Res* 3:163–172. <https://doi.org/10.1029/WR003i001p00163>
- Sperber KR, Annamalai H, Kang IS, et al (2013) The Asian summer monsoon: an intercomparison of CMIP5 vs. CMIP3 simulations of the late 20th century. *Clim Dyn* 41:2711–2744. <https://doi.org/10.1007/s00382-012-1607-6>
- Srinivasa Raju K, Sonali P, Nagesh Kumar D (2017) Ranking of CMIP5-based global climate models for India using compromise programming. *Theor Appl Climatol* 128:563–574. <https://doi.org/10.1007/s00704-015-1721-6>
- Teng J, Vaze J, Chiew FHS et al (2012) Estimating the relative uncertainties sourced from GCMs and hydrological models in modeling climate change impact on runoff. *J Hydrometeorol* 13:122–139. <https://doi.org/10.1175/JHM-D-11-058.1>

- Teutschbein C, Seibert J (2010) Regional climate models for hydrological impact studies at the catchment scale: a review of recent modeling strategies: regional climate models for hydrological impact studies. *Geogr Compass* 7:834–860. <https://doi.org/10.1111/j.1749-8198.2010.00357.x>
- Teutschbein C, Seibert J (2013) Is bias correction of regional climate model (RCM) simulations possible for non-stationary conditions? *Hydrol Earth Syst Sci* 17:5061–5077. <https://doi.org/10.5194/hess-17-5061-2013>
- Teutschbein C, Grabs T, Karlsen RH et al (2015) Hydrological response to changing climate conditions: spatial streamflow variability in the boreal region. *Water Resour Res* 51:9425–9446. <https://doi.org/10.1002/2015WR017337>
- Themeßl MJ, Gobiet A, Leuprecht A (2011) Empirical-statistical downscaling and error correction of daily precipitation from regional climate models. *Int J Climatol* 31:1530–1544. <https://doi.org/10.1002/joc.2168>
- Uniyal B, Jha MK, Verma AK (2015) Assessing climate change impact on water balance components of a River Basin using SWAT model. *Water Resour Manag* 29:4767–4785. <https://doi.org/10.1007/s11269-015-1089-5>
- Vicente-Serrano SM, Beguería S, López-Moreno JI (2010) A multiscale drought index sensitive to global warming: the standardized precipitation evapotranspiration index. *J Clim* 23:1696–1718. <https://doi.org/10.1175/2009JCLI2909.1>
- Visser H, Folkert RJM, Hoekstra J, de Wolff JJ (2000) Identifying key sources of uncertainty in climate change projections. *Clim Chang* 45:421–457. <https://doi.org/10.1023/A:1005516020996>
- Wang GQ, Zhang JY, Xuan YQ et al (2013) Simulating the impact of climate change on runoff in a typical river catchment of the loess plateau, China. *J Hydrometeorol* 14:1553–1561. <https://doi.org/10.1175/JHM-D-12-081.1>
- Wilby RL (2010) Evaluating climate model outputs for hydrological applications. *Hydrol Sci J* 55:1090–1093. <https://doi.org/10.1080/02626667.2010.513212>
- Wilby RL, Wigley TML (2000) Precipitation predictors for downscaling: observed and general circulation model relationships. *Int J Climatol* 20:641–661. [https://doi.org/10.1002/\(SICI\)1097-0088\(200005\)20:6<641::AID-JOC501>3.0.CO;2-1](https://doi.org/10.1002/(SICI)1097-0088(200005)20:6<641::AID-JOC501>3.0.CO;2-1)
- Wood EF, Lettenmaier D, Liang X et al (1997) Hydrological modeling of continental-scale basins. *Annu Rev Earth Planet Sci* 25:279–300. <https://doi.org/10.1146/annurev.earth.25.1.279>
- Xie Z, Yuan F, Duan Q et al (2007) Regional parameter estimation of the VIC land surface model: methodology and application to river basins in China. *J Hydrometeorol* 8:447–468. <https://doi.org/10.1175/JHM568.1>
- Xu Y, Gao X, Giorgi F (2010) Upgrades to the reliability ensemble averaging method for producing probabilistic climate-change projections. *Clim Res* 41:61–81. <https://doi.org/10.3354/cr00835>
- Yan D, Werners SE, Ludwig F, Huang HQ (2015) Hydrological response to climate change: the Pearl River, China under different RCP scenarios. *J Hydrol Reg Stud* 4:228–245. <https://doi.org/10.1016/j.ejrh.2015.06.006>
- Yang Z, Zhang Q, Hao X (2016) Evapotranspiration trend and its relationship with precipitation over the loess plateau during the last three decades. *Adv Meteorol* 2016:1–10. <https://doi.org/10.1155/2016/6809749>
- Zarch MAA, Sivakumar B, Sharma A (2015) Droughts in a warming climate: a global assessment of standardized precipitation index (SPI) and reconnaissance drought index (RDI). *J Hydrol* 526:183–195. <https://doi.org/10.1016/j.jhydrol.2014.09.071>
- Zhang JY, Wang GQ, Pagano TC et al (2013) Using hydrologic simulation to explore the impacts of climate change on runoff in the Huaihe River basin of China. *J Hydrol Eng* 18:1393–1399. [https://doi.org/10.1061/\(ASCE\)HE.1943-5584.0000581](https://doi.org/10.1061/(ASCE)HE.1943-5584.0000581)
- Zhou S, Chen J, Gong P, Xue G (2006) Effects of heterogeneous vegetation on the surface hydrological cycle. *Adv Atmos Sci* 23:391–404. <https://doi.org/10.1007/s00376-006-0391-9>
- Zhu C, Lettenmaier DP (2007) Long-term climate and derived surface hydrology and energy flux data for Mexico: 1925–2004. *J Clim* 20:1936–1946. <https://doi.org/10.1175/JCLI4086.1>